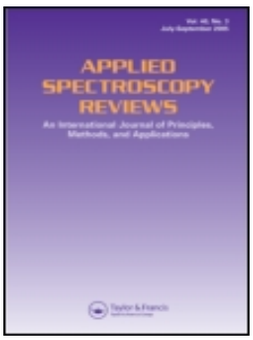

Applied Spectroscopy Reviews

ISSN: 0570-4928 (Print) 1520-569X (Online) Journal homepage: https://www.tandfonline.com/loi/laps20

Applications of Raman spectroscopy in detection of water quality

Zhen Li, Jinxing Wang & Daoliang Li

To cite this article: Zhen Li, Jinxing Wang & Daoliang Li (2016) Applications of Raman spectroscopy in detection of water quality, Applied Spectroscopy Reviews, 51:4, 333-357, DOI: 10.1080/05704928.2015.1131711

To link to this article: https://doi.org/10.1080/05704928.2015.1131711

Accepted author version posted online: 18 Dec 2015.
Published online: 04 Feb 2016.

Submit your article to this journal

Article views: 1074

View related articles

View Crossmark data

Citing articles: 12 View citing articles

Full Terms & Conditions of access and use can be found at
https://www.tandfonline.com/action/journalInformation?journalCode=laps20

APPLIED SPECTROSCOPY REVIEWS
2016, VOL. 51, NO. 4, 333–357
http://dx.doi.org/10.1080/05704928.2015.1131711

Taylor & Francis
Taylor & Francis Group

Applications of Raman spectroscopy in detection of water quality

Zhen Li[a,b,c,d], Jinxing Wang[b], and Daoliang Li[a,c,d]

[a]College of Information and Electrical Engineering, China Agricultural University, Beijing, China; [b]College of Mechanical and Electronic Engineering, Shandong Agricultural University, Taian, China; [c]Key Laboratory of Agricultural Information Acquisition Technology, Ministry of Agriculture, China Agricultural University, Beijing, China; [d]Beijing Engineering and Technology Research Centre for Internet of Things in Agriculture, China Agricultural University, Beijing, China

ABSTRACT

Water pollution is hazardous to the health of humans and other organisms, and detection of pollutants in aquatic environments is of primary importance for water quality monitoring. Raman spectroscopy offers an effective tool for qualitative analysis and quantitative detection of contaminants in a water environment. This article focuses on applications of Raman spectroscopy for detection of water quality. In this article, various Raman spectroscopy techniques employed for water quality detection are presented based on the types of pollutants: organics, inorganics, and biological contaminants. Additionally, the relevant detection parameters are reviewed, such as detection materials, limit of detection, detection range, peak positions, and selectivity. Furthermore, the advantages and limitations of various Raman spectroscopy techniques are summarized. Finally, the future development of Raman spectroscopy for detection of water quality is discussed.

KEYWORDS

Raman spectroscopy; water quality; detection; contaminants

Introduction

Fresh water is essential for human health, industry and agriculture. But currently, world water resources has been seriously contaminated (e.g., approximately 1.2 billion people lack access to safe drinking water) due to natural effects and large-scale patterns of human activities (1–3). In general, water quality can be broadly characterized by concentrations of microbiological, organic and inorganic contaminants as well as indicators such as pH, conductivity, dissolved oxygen, etc. (4). Recently, the negative influences of water pollution on the human body and sustainable development of human society (such as industry and aquaculture) have attracted increasing attention. Therefore, a variety of methodologies have appeared for the detection of pollutants in a water environment (5).

The traditional methods applied for water quality detection (6) involve enrichment analysis, volumetric analysis (7), electrochemical analysis (8), spectrophotometry (9), emission spectrum analysis, fluorometric spectroscopy (10), atomic absorption spectroscopy (AAS) (11), infrared spectroscopy (12), and chromatography (13). In past decades, these traditional

CONTACT Daoliang Li dliangl@cau.edu.cn College of Information and Electrical Engineering, China Agricultural University, Beijing 100083, China.

© 2016 Taylor & Francis Group, LLC

technologies have been widely used for detection of pollutants in water, but many disadvantages still exist, such as low precision, long detection time and limited research fields.

Raman spectroscopy has emerged as a progressive method for detection of materials in water environments and might be able to make up for the deficiencies of the other detection technologies. The Raman spectrum is a type of scattering spectrum, and Smekal et al. (14) first theoretically predicted the existence of Raman effects in 1923. Based on the Raman scattering effect, the analysis method used in Raman spectroscopy was first discovered by Indian physicist C.V. Raman in 1928 (15). Furthermore, Raman spectroscopy was first used in 1970 to detect organic contaminants in water (16). However, this method was not widely investigated prior to the 1980s due to the low Raman scattering efficiency. In recent years, Raman spectroscopy has been combined with variety of advanced techniques and has developed into an excellent and effective tool for detection of pollutants in a water environment due to its high precision and detection efficiency, non-destructive sampling capability, and minimal sample preparation (17, 18). For instance, the use of optical fibers could enable the use of a Raman spectrometer located far away from the detected materials to allow remote and online detection of specific materials in water (19); Micro-Raman spectrometry provides micrometre-scale analysis with spectral resolutions of up to 1 cm^{-1} (20).

The aim of this article is to review applications of Raman spectroscopy for detection of water quality. This article includes various Raman spectroscopy techniques applied for the detection of different types of contaminants in water environments. It is organized based on the type of detected materials, including organics, inorganics, and biological pollutants. Moreover, this article provides a broad summary of research findings that use Raman spectroscopy for detection of pollutants in an aqueous environment together with their characteristic properties. It is intended as a guide for further studies that concentrate on detection of other contaminants using Raman spectroscopy, particularly ammonia nitrogen.

Raman spectroscopy concepts

Principles

Light creates elastic scattering and inelastic scattering when it is used to illuminate samples. Inelastic scattering has components shorter than the excitation wavelength (21), and this phenomenon is collectively known as Raman effects. When this process occurs in elastic scattering (Rayleigh scattering), no energy is exchanged between molecules and photons (22). If the process occurs in inelastic scattering, energy is exchanged between molecules and photons, which is known as Raman scattering (23).

The interaction of incident light with the vibrational modes in a sample (such as a solid, gas or liquid) causes losses and gains of energy in the incident beam, which are known as Stokes and anti-Stokes scattering, respectively (24). As shown in Figure 1, a Rayleigh scattering line has the highest intensity (approximately 10^{-3} times as high as that of the incident light), whereas an anti-Stokes line is not easily observed due to the weaker intensity of an anti-Stokes line compared with that of a Stokes line. In other words, most photons of incident light are Rayleigh scattering without energy change (25–27). From the figure, we observe that the Raman spectrum is a plot that describes the wavelength relative to scattering intensity and Raman shift (Δv cm^{-1}). Additionally, each material has its own unique Raman spectra lines, and the Raman frequency shift (frequency variation) refers to the vibrational

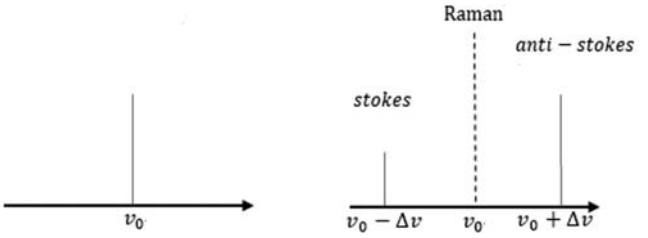

Figure 1. Raman, Stokes, and anti-Stokes lines.

levels of the molecules. The peaks in the spectrum (the intensity of the Raman spectra) are related to the concentration of substances such that Raman spectroscopy can be applied for quantitative detection of contaminants in a water environment (28).

Instrumentation

Generally, a Raman spectrometer consists of five components, as shown in Figure 2: an excitation source, light collection system, monochromator, detector, and data processing system (29). From the figure, we note the fundamental operational principle (18).

Excitation source

As a component of the spectrometer, the excitation source plays an important role in the performance of a Raman spectrometer. The function of the excitation source is to provide

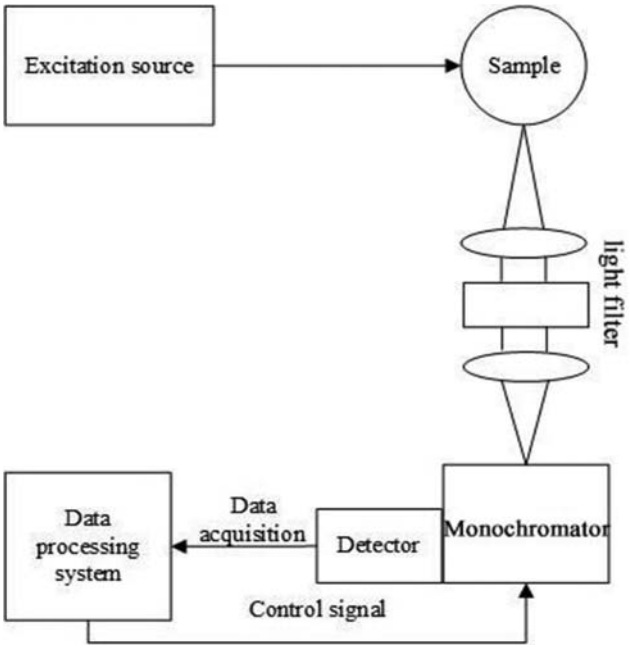

Figure 2. An ordinary Raman spectrometer.

highly monochromatic, powerful and multi-wavelength incident light, and thus, two significant parameters of the excitation source are its bandwidth and power. Currently, the excitation source used in Raman spectroscopy is a laser instead of a mercury lamp, as used in the past. As stated, the frequency shift between the excitation signal and the Raman signal is related to the fundamental vibrational frequency of a molecule. Therefore, a narrow bandwidth or a highly monochromatic beam with high power is preferred for stability and sufficiently high intensity of the Raman spectrum. (30) The common types of lasers and wavelengths are listed in Table 1 (31–33).

Monochromator

The monochromator is used to separate the Raman scattering light by wavelength and is the most critical component in a Raman spectrometer. A Raman spectrometer requires a high stray level because of the weak intensity of Raman spectroscopy. Particularly, the limitation of the grating is the main source of stray light in a Raman spectrometer. Generally, dispersive (34) and non-dispersive are the two basic types of monochromator. A Fourier transform Raman (FT-Raman) spectrometer (non-dispersive spectroscopy) is composed of a multiplexing spectrometer system, such as a Michelson interferometer, whereas dispersive Raman spectroscopy uses gratings and multistage monochromators to determinate the radiation scatter of a sample (35) (Figure 3).

Detector

The function of the detector is to collect the information from the spectrum, and the data are subsequently serially input into the computer via data acquisition. The detector should be sensitive due to the low Raman scattering efficiency, which could have a negative effect on the detection of the Raman signal (30). Generally, the received types of Raman scattering signal can be divided into single-aisle (e.g., photomultiplier tubes (PMT)) and multi-aisle (e.g., charge-coupled device (CCD)).

A PMT is composed of a photoelectric emission cathode, focusing electrode, electron multiplier, and anodes. The photoelectrons are excited into a vacuum by the photocathodes, and the light is used to illuminate the photocathodes. These photoelectrons then enter into a multiplication system via the focal electric field and are amplified by the multiplication obtained by the secondary emission. Finally, the amplified electrons are collected by the anode as the output signal. Compared with other types of detectors, PMTs offer a number of advantages, such as higher gain, lower noise level, and shorter transit time.

However, with the emergence of CCD detectors first presented by Murray et al. (36) in the 1980s, PMT detectors have gradually faded from use in Raman spectrometers. The fundamental structure of a CCD detector consists of a metal-oxide-semiconductor diode on a thin silicon substrate (37, 38). The advantages of CCD detectors are their specific function

Table 1. Common types of lasers.

Laser types	He:Ne	Argon ion	Krypton ion	He:Cd	Nd:YAG	Diode lasers
Wavelength	632.8 nm	458.0, 488.0, 514.5 nm	530.9, 647.1 nm	441.6 nm	1064, 532 nm	630, 780 nm

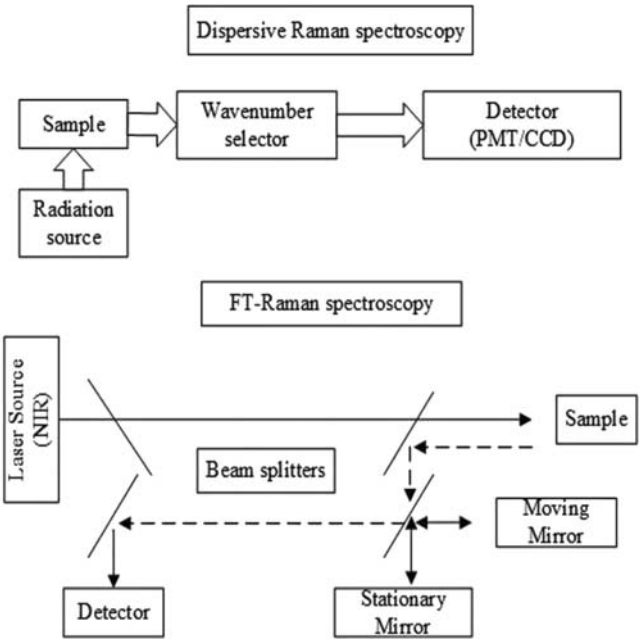

Figure 3. Schematics of FT-Raman and dispersive Raman systems (35). Reprinted with permission of Elsevier. Permission to reprint must be obtained from the rightsholder.

image sensing and self-scanning, high sensitivity, low detection noise, multichannel characteristics, and high quantum efficiency. Furthermore, many other detectors have been used in a Raman spectrometer, including silicon avalanche photodiode (APD) (39, 40) detectors and NIR detectors.

Data processing system

Data processing can be a complicated process, and data processing technology is crucial due to the large amount of data collected by the detectors. Commonly, the electronic processing methods applied for extraction of the information from Raman scattering include DC amplification, frequency selection, and photon counting, and the spectrum is drawn by a recorder or computer software. In the data processing system, the bandwidth of the telephone line and network is one of the most critical limiting factors. Therefore, the data from a Raman spectrum should be compressed into small data sets. Moreover, it is known that useful information cannot be extracted from the collected data in the analysis of the spectrum due to noise, and thus, data processing is essential for a Raman measurement and the techniques usually include data compression and filtering de-noising.

The wavelet transform was first employed for analysis of seismic data in 1984, as presented by Morlet (41), a French earth physicist. The main spectral signature of interest is the shape, size, and position of the Raman characteristic peak in the analysis of spectrum, which is the local characteristic of chemical signals. There have been many reports demonstrating that the wavelet transform is suitable for analysis of the local characteristics of signals. Currently, the wavelet transform is primarily applied in de-noising and compression of signals due to its distinct advantages for analysing the spectrum. Thus, the wavelet transform

method offers an effective tool for processing of spectral data (signal de-noising and data compression) in a Raman spectroscopy system.

Application of Raman spectroscopy in detection of water quality

Currently, the existing Raman spectroscopy technologies include normal Raman spectroscopy, resonance Raman scattering (RRS) (42), surface-enhanced Raman scattering (SERS) (43), FT-Raman spectroscopy (44), and their combination technology. Raman spectroscopy has widely been used for the detection of pollutants in the water environment, and the existing research results are listed in Table 2.

Organics

Polycyclic aromatic hydrocarbons

Polycyclic aromatic hydrocarbons (PAHs) are a type of organic compound that are known as carcinogenic pollutants and are composed of two or more condensed aromatic rings. It is notable that relatively few studies focus on the detection of polycyclic aromatic hydrocarbons (PAHs) using Raman spectroscopy, particularly surface-enhanced Raman spectroscopy (47, 48).

PAHs in seawater have become an ongoing concern due to their high carcinogenic and mutagenic activities. In this field, Schmidt et al. (49) presented a detection method for aromatic hydrocarbons in seawater using sol-gel-derived SERS substrates. In this work, Schmidt concentrated on quantitative analysis of PAHs in seawater and detection of multiple-component PAH mixtures with the ability to detect low-concentration PAHs, and its limits of detection rang from ppb to ppt. The experiments studied a mixture of five dissolved PAHs in seawater and demonstrated the effectiveness of this method. Additionally, it was shown that the detection limits of the PAH concentration in seawater were improved by increasing the enhancement factors of the substrates and the enrichment properties of the SERS surface.

Costa et al. (50) studied the chemical detection of PAHs by SERS in aqueous solutions. In this work, he studied the development of SERS-active substrates that are specific for characterization and spectroscopic study of PAHs, i.e., instead of the traditionally prepared Au films, metal nanomaterials were used in the development of sensitive chemical methods of detection and identification of PAHs using Raman spectroscopy. The utility of coated Au films was demonstrated as a robust SERS substrate for detection and identification of PAHs and nitro-PAHs. The method employed in this work did not require previous extraction (for

Table 2. Pollutants in water that can be detected using Raman spectroscopy.

Types of pollutants	Pollutants
Organics (45)	Benzene, phenol, aldehyde, carbon tetrachloride, polycyclic aromatic hydrocarbon glucose, quinoline, cilia, methyl derivative, aromatic compounds with nitrogen, edible oil, pesticide, organic dye, synthetic detergent, gasoline and its derivatives and biomacromolecule.
Inorganics (46)	Chlorate, hypochlorite and perchlorates, heavy metals (e.g., mercury, lead, chromium and arsenic), cyanide, ferricyanide, nitrate, nitrite, asbestos and sulfate.
Others	Bacteria, viruses and microbial pathogens

which the extraction phase occurs in the SERS platform) or separation methods, did not require the use of organic solvents, and was capable of simultaneously detecting and identifying a number of compounds. This method also demonstrated that it allows detection of trace concentrations in aqueous solutions and enabled the simultaneous detection of PAHs using Raman spectroscopy at ppm levels in the aqueous environment.

Xie et al. (51) found that substrates made of gold nanoparticles modified with cyclodextrin could be replaced by thiols. Based on SERS, a mixture of five dissolved PAHs (anthracene, pyrene, chrysene, triphenylene and coronene) was qualitatively identified and quantitatively detected using this method. The detection limits for each PAH (anthracene, pyrene, chrysene, and triphenylene) were found to be 100, 10, 100, and 1000 nM, respectively. In addition, the experiments studied the coverage rate of the surface of gold nanoparticles modified by thiols and the effect of centrifugal speed on the results of the detection. The fundamentals of interaction between the SERS substrate modified by thiol to replace the cyclodextrin and PAHs is the same as that of calixarenes.

Surface-enhanced Raman spectroscopy coupled with a calixarene-modified substrate could be employed for the detection of PAHs. Sanchez-Cortes et al. (47, 52–54) researched this topic and reported certain achievements. Shi et al. (55, 56) studied a substrate made of silver nanoparticles and gold sol film modified by 25, 27-dimercaptoacetic acid-26 and 28-dihydroxy-4-terbutyl calix [4] arene (DMCX), which are derivatives of calixarene. The limits of detection for pyrene and anthracene in an artificial sea could reached 3×10^{10} M and 13×10^{9} M using this substrate. The response time between pyrene and the substrate was only 15 min, and the concentration of pyrene was in the range of 0-4×10^{7} M. With the use of DMCX-functionalized gold colloid film combined with application of the shifted excitation Raman difference spectroscopy (SERDS) technique, the limit of Raman signals of pyrene and anthracene in aqueous solutions could reach a notably low concentration level (approximately 0.5 M) (55). This article provided a high sensitive and selective method for the in-situ detection of PAHs.

Qu et al. (57) restored silver nitrate using humic acids (HAs) and modified reduced silver nanoparticles. The HAs-Ag nanoparticles exhibited high SERS activity and strong adsorption of aromatic hydrocarbons under the reaction of π-π with a good stability for the loose network structure produced by HAs surrounding the nanoparticles, which prevented polymerase activity of nanoparticles. Later, Lopez-Tocon et al. (58) detected PAHs through assembling lucigenin of biacridine bivalent dication to silver nanoparticles, and the method effectively detected PAHs and different numbers of fused benzene rings which consist of pyrene, benzophenanthrene, benzo [c], and coronene. The results of this experiment demonstrated the high selectivity of the substrate modified by thiol.

Benzene

Benzene in the form of industrial chemicals could cause serious damage to the central nervous system and bone marrow of the human body. The main method employed for detection of benzene is chromatography, which is complicated to operate and requires high temperature stability. Many reports are available on Raman spectroscopy applications for the detection of benzene.

Leslien et al. (59) examined the Raman spectra of benzene and toluene under a fairly high dispersion of 4-5 A. per mm. In this work, it was revealed that the line in the neighborhood

of 1000 cm^{-1}, which is always characteristic of the benzene ring, was complex. Five components were found in benzene: 1005.3 cm^{-1}, 998.8 cm^{-1}, 992.2 cm^{-1}, 983.9 cm^{-1}, and 980.3 cm^{-1} and toluene contained four frequencies in this region: 1027.7 cm^{-1}, 1001.9 cm^{-1}, 992.2 cm^{-1}, and 968.3 cm^{-1}. In addition, several other lines obtained in this experiment were observed to be complex, and a number of entirely new lines were observed in toluene. Overall, this research set the stage for the detection of benzenes in the water environment.

Liu et al. (60) studied the laser Raman spectra of benzene and carbon tetrachloride, and the spectrometer used in the experiment was a LRS-II/III laser Raman spectrometer. The study showed that benzenes could be identified in mixed solutions via analysis and research on the Raman spectra of benzene, carbontetrachloride and their mixed solutions. Additionally, it was found that the volume ratio of benzene and carbon tetrachloride approximately has a linear relationship compared with the intensity of the characteristic peaks, as analyzed by fitting the straight lines. The results demonstrated that the Raman characteristic peak with the highest intensity in the Raman spectra was located at 561 nm, corresponding to the symmetric vibration of benzene. The study provided a suitable method for qualitative and semi-quantitative detection of benzene in aqueous solutions.

Ma et al. (61) studied low-concentration detection of benzene using laser Raman spectroscopy in water environments. A total of 25 samples of benzene with different concentrations were studied using laser Raman spectroscopy technology. The results show that a linear relationship exists between the intensity of the Raman spectrum and the concentration of benzene in the range of 0.264–184.8 ppm. The linear correlation coefficient ($r = 0.99626$) was obtained using the least squares method, and the detection limit was 223 ppm. This research with a large range of concentrations and excellent linearity of data provides an effective analysis method for low-concentration detection of benzene.

In addition, Huang et al. (62) obtained the Raman vibration spectrum of color-benzene using laser Raman spectroscopy and analyzed the characteristics of Raman spectroscopy of color-benzene and the reason of presenting the rules to form a theoretical basis for detection of color-benzene in organics. Tao et al. (63) studied the relationship between the intensity of the spectrum and the concentration of benzene in the concentration range of 0.3–60%. Based on theoretical analysis of the benzene Raman spectrum, the experiments proved that the Raman spectrum peak value of benzene was proportional to the concentration of benzene, which could be obtained by substituting the strongest peak value of 561.4 nm into the linear regression equation, and the detection limit was 0.3%.

Antibiotics

Antibiotics in the water environment primarily originate from industrial wastewater, medical antibiotics, and veterinary antibiotics, and antibiotics in aquaculture accounted for a large proportion of the antibiotics. The phenomenon of antibiotic abuse in aquaculture has existed for several years. Even trace amounts of antibiotics could cause serious and potential harm to the body due to cumulative effects.

Based on the theory of density functions, Lliescu et al. (64) of Romania simulated the Raman characteristic peak of potassium benzylpenicillin. The results demonstrated that the main characteristic peak of potassium benzylpenicillin included deformation vibrations of the benzene ring at 388 cm^{-1} and 451 cm^{-1}, stretching vibration of the triangle ring at 985 cm^{-1}, C-C stretching vibration at 1005 cm^{-1}, breathing vibration of the benzene ring at

1032 cm^{-1}, and a C-N-C stretching vibration. The SERS spectrum of a potassium benzylpenicillin solution was obtained in the experiment using a substrate made of silver sol, and it was demonstrated that shifts of the main characteristic peak occur at 385 cm^{-1}, 458 cm^{-1}, 980 cm^{-1}, 1000 cm^{-1}, 1028 cm^{-1}, and 1600 cm^{-1}. By comparison, the results simulated using the theory were similar to the detected results obtained in experiments.

He et al. (65) reported rapid detection of antibiotics via SERS using a dendritic silver nanosubstrate in aqueous environment. In this study, based on the silver nanosubstrate, SERS methods with near-IR excitation at 785 nm were employed for detection of three restricted antibiotics (i.e., enrofloxacin, ciprofloxacin, and chloramphenicol), which were prepared in standard solutions prior to the experiments. It was found that SERS was capable of identifying and characterizing the three antibiotics quickly and accurately using the dendritic silver nanosubstrate, which displayed stable and satisfactory performance in detection and analysis of trace amounts of antibiotics in a water environment. And the limit of detection for the antibiotics reached the level of 20 ppb.

SERS coupled with silver sol film substrates was used in a study of rapid detection and characterization of antibiotics in an aqueous environment performed by Ma et al. (66). The experiments studied the effects of the pH value of silver colloids applied (via a self-assembly method) as a coating film and the coating times on the performance enhancement of antibiotic detection. Meanwhile, based on SERS, three antibiotics (chloramphenicol, ciprofloxacin and enrofloxacin) were detected in an aqueous environment using the most suitable substrates. The results showed that the silver sol film exhibited a highest satisfactory enhancement factor for antibiotics while the pH of the silver colloid was 4, and the time for coating films was 5. The lower concentration limits of detection for chloramphenicol, ciprofloxacin and enrofloxacin reached 120 nM, 15 nM, and 120 nM, respectively. Additionally, the results obtained in the experiment indicated that silver sol films with high sensitivity had vital application value in the field of rapid and in-site trace detection of antibiotics in a water environment.

Pesticides

Pesticides can harm aquatic organisms in aquaculture and the surrounding water environment due to abuse of pesticides used on crops. Although it is known that pesticides are essential in agricultural production, pesticide residues on crops and in aquatic organisms will bring some negative influences on humans. Organophosphates are the most common pesticide residues found on food and include dichlorvos, organochlorines such as toxaphene, carbamate (e.g., Carbofuran), and pyrethroid esters. In addition, the phenomenon of abuse of pesticides in aquaculture has become more serious and presents a considerable threat to humans.

SERS with substrates made of gold nanorods modified by cyclodextrin was employed for detection of carbendazim in benzimidazole fungicides studied by Strickland et al. (67). The results demonstrated that the limit of detection could reach 50 mM with quantitative analysis of the data using the particle least squares method. Wang et al. (68) quantitatively detected carbaryl using substrates composed of Si nanowires modified by silver nanoparticles based on the SERS method, and the sensitivity of detection reached 10^{-17} M.

White et al. (69) designed a flowing SERS micro-system without a pump and used it for detection of three fungicides (methyl parathio, malachite, and thiram) in aquaculture water.

The system was composed of a pipette, microporous, glass tube, excitation optical fiber, collection fiber, and a portable spectrometer laser. In this experiment, porous models made from quartz powder modified by 3-MTS were installed in the glass tube, and both the excitation fiber and collection fiber were aimed at the glass tube. The silver sol prepared using the Lee-Meisel method was mixed evenly into the solution, and the mixed solution was then placed in the liquid inlet. The procedure for detection involved the flow of the mixed solution in the glass tube through a microchannel after the pipette was pulled, and the mixed solution was adsorbed on the quartz powder, and the solution was subsequently detected. This work showed that the minimum detection concentrations of the three fungicides were 5 ppm, 0.1 ppb, and 1 ppb. The flowing SERS micro-system would be significant for application value in the field of real-time detection of pesticides.

Kubackova et al. (70) used surface-enhanced Raman spectroscopy and optimization of the SERS-sensing substrate for detection of the organochlorine pesticides aldrin, dieldrin, lindane, and α-endosulfan in aqueous solutions. In this work, a functionalization of metal nanoparticles was carried out by using aliphatic $\alpha\omega$-dithiols as bifunctional linkers in order to create a suitable environment for assembly and SERS detection of analyzed pesticides. The results confirmed high sensitivity of surface-enhanced Raman spectroscopy for detection of the organochlorine pesticides with a limit of detection reaching 10^{-8} M.

Others

There also have been many reports published on Raman spectroscopy applications for the detection of other organics in water environments. Marley et al. (71) studied the detection of 2-, 3-, and 4-nitrophenols using resonance Raman spectroscopy. The data obtained showed that the limits of detection were 30, 400, and 70 ppb for 2-nitro-, 3-nitro-, and 4-nitro-, respectively, using the 458-nm line of an argon-ion laser.

Additionally, Si et al. (72) reported an article based on SERS coupled with silver nanoparticles prepared using an electrolysis method, transmission electron microscopy (TEM), and scanning electron microscopy (SEM) that could be used for the detection of three types of azo-dye in aqueous solutions, including Methyl Yellow, Methyl Red, and Sudan Red 1. The experimental results showed good agreement with the calculation results obtained using Gaussian'98 software. It was also found that the limit of detection for azo-dye could be down to 10^{-5} M in aqueous solutions. Moreover, Tanner et al. (73) reported a result on the detection of organophosphorus pesticides (OOPs) using FT-Raman spectroscopy. The study showed that the limit of detection was 39 ppm for O, O-dimethyl-O-2, 2-dichlorovinylphosphate (DDVP), with a P-(O-C) stretch at 1051 cm^{-1}. It was also demonstrated that FT-Raman spectroscopy could be a useful tool for the detection of OOPs.

As shown in Table 3, various types of organics have been investigated, and the detection parameters and performances are summarized from the above studies, including the detection method, limit of detection, detection range and the peak positions.

The methods described above have demonstrated that Raman spectroscopy could be successfully employed for detection of organics in a water environment. These results show that the limit of detection could reach the level of ppm. Additionally, as one of the Raman spectroscopy techniques, SERS has been widely used for the detection of

Table 3. Detection parameters and performance of organics in water using Raman spectroscopy.

Detection materials	Method	Limit of detection	Detection range	Peak positions	Reference
Polycyclic aromatic hydrocarbons	Surface-enhanced Raman spectroscopy	ppt	ppb to ppt	N/A	(49)
		Anthracene: 100 nM Pyrene: 10 nM Chrysene: 100 nM Triphenylene: 1000 nM	Anthracene: 10^{-4}-10^{-7} M Pyrene: 10^{-4}-10^{-8} M Chrysene: 10^{-4}-10^{-7} M Triphenylene: 10^{-4}-10^{-6} M	Anthracene: 392, 1256 and 1536 cm^{-1} Pyrene: 1062, 1238, and 1625 cm^{-1}	(51)
		Pyrene: 3×10^{-10} M Naphthalene: 13×10^{-9} M	Pyrene: 5×10^{-10}-4×10^{-7} M	Pyrene: 1234 cm^{-1} Anthracene: 1377 cm^{-1}	(56)
	Shifted excitation Raman difference spectroscopy	Pyrene and Anthracene: 0.5 M	Pyrene: 0.5-400 nM Anthracene: 0.5-80 nM	Pyrene: 588, 1235, and 1401 cm^{-1} Anthracene: 750, and 1001 cm^{-1}	(55)
Benzene	Laser Raman spectroscopy	223 ppm	184.8-0.264 ppm	996.7 cm^{-1},	(61)
		0.3%	Mass fraction: 60-0.3%	N/A	(62)
Antibiotic	Surface-enhanced Raman spectroscopy	Ciprofloxacin: 20 ppb;	Ciprofloxacin: 20 ppb-200 ppm	Ciprofloxacin: 1392 cm^{-1}	(65)
		Chloramphenicol: 120 nM Ciprofloxacin: 15 nM Enrofloxacin: 120 nM	Chloramphenicol: 120-1.92 nM Ciprofloxacin: 15-960 nM Enrofloxacin: 120-1.92 nM	Chloramphenicol: 1354, and 1602 cm^{-1} Ciprofloxacin: 1390 cm^{-1} Enrofloxacin: 1387 cm^{-1}	(66)
Pesticide	Surface-enhanced Raman spectroscopy	Carbendazim: 50 mM	Carbendazim: 10^{-4}-10^{-5} M;	Carbendazim: 1007, and 1242 cm^{-1}	(67)
		Carbaryl: 0.02 ppm;	Carbaryl: 10^{-2}-10^{-7} M	Carbaryl: 1378 cm^{-1}	(68)
		Methyl parathion: 5 ppm	N/A	Methyl parathion: 844, 1100, 1153, 1337, and 1583 cm^{-1}	(69)
		Malachite: 0.1 ppb		Malachite: 902, 1162, 1208, 1286, 1359, 1387, 1585, and 1614 cm^{-1}	
		Thiram: 1ppb		Thiram: 911, 1133, 1375, 1430, and 1508 cm^{-1}	
	Fourier transform Raman spectroscopy	DDVP: 39 ppm	N/A	DDVP: 1051 cm^{-1}	(73)
Phenols	Resonance Raman spectroscopy	2- nitrophenol: 30 ppb 3-nitrophenol: 400 ppb 4-nitrophenols: 70 ppb	N/A	N/A	(71)
Azo-dye	Surface-enhanced Raman spectroscopy	Methyl Yellow, Methyl Red, Sudan Red: 10^{-5} M	N/A	Methyl Yellow: 1137, 1377, and 1597 cm^{-1} Methyl Red: 1121, 1178, and 1374 cm^{-1} Sudan Red: 999, 1175, and 1150 cm^{-1}	(72)

organics in water. However, future studies should focus on increasing the activity of SERS substrates or finding more suitable substrates to enhance the limit of detection, precision and stability. It is obvious that the method described above is applicable to the detection of organics, but Raman spectroscopy also could be used for the detection of inorganics in water.

Inorganics

Perchlorate

In recent years, much interest has been focused on developing new technologies for qualitative and quantitative analysis of perchlorate ions (ClO_4^{-1}) in the environment since perchlorate ions emerged as a widespread contaminant in the water environment (74–76). Perchlorate ions also have been detected in drinking water, plants, food products and aquaculture. A portion of perchlorate is manufactured, but naturally formed perchlorate is widespread. It is well known that perchlorate ions can harm not only human health but also the environment.

Ruan et al. (77) presented a new methodology based on the SERS method that used a substrate composed of 2-dimethyl-aminoethanethiol (DMAE) modified by gold nanoparticles for rapid and quantitative detection of perchlorate in a water environment. The results showed that the most intense characteristic Raman peak of ClO_4^- ions in aqueous solution occurs at 934 cm^{-1}, which is consistent with literature data for both normal and SERS methodologies, and the detection limit can reach 0.1 ppb in aqueous solution. This was the first time that DMAE was used as a modifier for SERS detection of ClO_4^-. Additionally, the experiments demonstrated that surface modification of Au nanoparticles with DMAE enables high sensitivity as well as good reproducibility in detecting ClO_4^- in aqueous solution. The methodology used in this work coupled with a portable Raman spectrometer might be suitable for real-time, quantitative and in situ detection of perchlorate ions in an aqueous environment.

Based on surface-enhanced Raman spectroscopy, Hao et al. (78) used Ag nanofilms deposited on Cu foils (Ag-Cu films) for the first time as substrates in rapid and sensitive sensing detection of perchlorate in aqueous solutions. This observation was similar to that from DMAE-modified gold nanoparticles as a SERS substrate for perchlorate SERS analysis. It was demonstrated in the experiments that the sizes and shapes of the nanoparticles could have a significant influence on the enhancement effects for perchlorate. Additionally, the experiments showed that Ag particles with a size of approximate 90 nm yielded the highest SERS enhancement. The results also showed that the limit of detection was determined to be as low as 5 ppb for ClO_4^-. This work provided an effective methodology for rapid and quantitative detection of aqueous perchlorate.

Additionally, the study by Li et al. (79) reported that silver nanoparticles (particle diameters of 30–40 nm) were produced using a chemical reduction method with steady properties and better dispersibility. It was found in the experiment that SERS coupled with the silver nanoparticle substrate could be used for rapid and accurate detection of ClO_4^- in perchlorate ion solutions with a low concentration range (10^{-3} to 10^2 ppm), and the limit of detection could reach as low as 10 ppb. The results showed that with the decrease of the ClO_4^- ion concentration, the intensity of SERS would be gradually weak at concentrations ranging from 10^{-2} to 10^2 ppm in perchlorate ion solutions.

Heavy metals

Heavy metals, such as mercury, cadmium, lead, chromium, and copper, are widely distributed in the environment and mainly originate from the discharge of industrial wastewater. These substances can cause a variety of human diseases, particularly cancers, due to their heavy toxicity, long residual time, and fast diffusion velocity (80). Moreover, heavy metals in water environments could accumulate in aquatic organisms even at low concentrations because they are difficult to degrade. And there are many reports existing of highly sensitive and versatile systems for detection of trace amounts of toxic heavy metals (81).

Witte et al. (82) reported that $CuIn_{1-x}Ga_xSe_2$ (CIGS) thin films with variable Cu contents were analyzed by Micro-Raman spectroscopy in the premise of the constant Ga/(Ga and In) ratio ($x = 0.3$). All of the results showed that the frequency of the Raman spectrum decreased with the increasing of copper content and gradually approached a minimum value. Additionally, changes in the contents of Cu caused changes in the peak widths and peak displacements, which provided a theoretical basis for feasibility of detection of heavy metal ions using Raman spectroscopy.

Mercury is widely considered to be one of the most toxic pollutants in the water environment. Wang et al. (83) reported a new methodology combining a droplet microfluidic chip and SERS technology employed for trace detection of mercury (II) ions (Hg^{2+}) in a water environment. The results of the experiments demonstrated a rapid and sensitive detection method for Hg^{2+} using SERS combined with droplet-based microfluidics. Based on the principles (the strong affinity between AuNPs and mercury (II) ions) of this method, changes in the SERS signal of rhodamine B molecules were monitored. A linear relationship between the concentration of Hg^{2+} in aqueous solutions and the SERS intensity of rhodamine B molecules was found in the experiments. Quantitative detection of mercury (II) ions was performed by calculating the spectral peak area of rhodamine B molecules at 1647 cm^{-1}. The calculated concentration showed a good linear relationship in the concentration range of 0.1–2.0 ug/L, and the limits of detection were approximately between 100 and 500 ppt. The methodology proposed in this article provided the ability to detect traces of Hg^{2+} rapidly and reproducibly in a water environment.

Li et al. (84) adopted reduced glutathione hormone (GSH) functionalized silver nanoparticles, and their experiments also used silver nanoparticles labeled with 4-mercaptopyridine as Raman markers. The As^{3+} were placed into the basement, and a Raman spectrum was produced by aggregation of silver nanoparticles due to the connection of GSH and As^{3+}. The results of the experiment suggested that the limits of detection for As^{3+} could reach 0.76×10^{-6} ppm using the above methodology, and its practicability was verified through detection of As^{3+} in drinking water samples.

Furthermore, the study reported by Eshkeiti et al. (85) found that a novel substrate designed using inkjet printing of Ag nanoparticle ink on a Si wafer could produce enhanced Raman effects for detection of toxic heavy metals, e.g., cadmium sulfide (CdS), mercury sulfide (HgS), and zinc oxide (ZnO). The results demonstrated the feasibility of this novel SERS substrate applied in detection of toxic heavy metals, such as CdS, HgS, and ZnO.

Sulfate

Sulfate, which is widespread in sewage, industrial wastewater, and pesticide residues, poses a great threat to aquatic organisms and human health. However, the discarded solutions produce a large amount of salts (ammonium thiocyanate, ammonium thiosulfate, and ammonium sulfate) that are left over after desulfurization, decyanation, and purification methods in a coke oven gas, which have been demonstrated to be harmful.

An immense number of related papers have reported on applications for detection and analysis of SO_4^{2-} in aqueous solutions and the water environment using laser Raman spectroscopy. For instance, it was reported in the review published by Burke (24) that the work studied the Raman spectrum of a variety of ions and molecules with the use of Raman micro-spectrometry, including SO_4^{2-} ($\Delta v = 983\ cm^{-1}$), HSO_4^- ($\Delta v = 1050\ cm^{-1}$), and HS^- ($\Delta v = 2574\ cm^{-1}$) etc. Additionally, the results in this article reported the parameters for Raman frequency shift and Raman scattering cross-section, and a correlation analysis was performed according to the different situation of inclusions. A related study reported by Dubessy et al. (86) obtained Raman spectrum parameters in aqueous solution, and the experiments demonstrated a linear relationship between the intensity of the Raman spectrum and the concentration of the corresponding ions.

A Raman spectrum was obtained through study and analysis performed by Sun et al. (87) on an ammonium sulfate solution using laser Raman spectroscopy. It was shown that the Raman spectrum of ammonium sulfate had 4 obvious Raman characteristic peaks, and the shifts of the peaks were 448 cm^{-1}, 616 cm^{-1}, 980 cm^{-1}, and 1104 cm^{-1}. The strongest Raman intensity was due to the S-O symmetric stretching vibration, which occurred at 980 cm^{-1}. These detection data was obtained by comparing the experimental results based on analogue calculations and optimization of the geometry using the Hartree-Fock method and the Gasussian 03 software package. The results were consistent with the results of the theoretical calculations and indicated that a good linear relationship existed between the concentration of SO_4^{2-} and the intensity of the Raman spectrum. The methodology used in this article is simple and convenient for Raman spectrum detection of ammonium sulfate solution, and the results provide a reference for identification and quantitative detection of sulfate in actual production. Similarly, Zou et al. (88) studied quantitative detection of common acid radical ions (e.g., Cl^-, SO_4^{2-}, and acetic acid ions) in micro-solution from fluid inclusions using laser Raman spectroscopy. The results in the study showed that laser Raman spectroscopy could be used for quantitative detection of common acid radical ions.

Based on Raman spectroscopy, Deng et al. (89) designed a reaction device for gas hydrate and applied it for quantitative detection of SO_4^{2-} in seawater. The results showed a good linear relationship for the Raman spectrum parameters in the concentration range of 2×10^3-7×10^4 ppm. The related correlation coefficient was $R = 0.9998$, and the detection limit was 200 ppm (approximately 238 μg/ml). The results also demonstrated that laser Raman spectroscopy could be used for rapid, real time, and quantitative detection of sulfate in seawater, an environment with high temperature and low pressure. Compared with ion chromatography, the Raman spectroscopy methodology could be used on the original samples and was fast and convenient.

Nitrate

Nitrate, a widespread environmental contaminant, has been discovered in nature, particularly in vaporous water, surface or groundwater, aquaculture water, the bodies of plants and animals, and food. As nitrates continue to enter aquatic systems from anthropogenic sources, accelerated eutrophication occurs in fresh water and marine ecosystems (90, 91). Elevated nitrate concentrations cause methemoglobinemia in aquatic animals (92) and blue baby syndrome in human infants (93).

In the study by Lombardi et al. (46), Raman spectroscopy was employed for detection of several nitrates, nitrites, and sulfates, both in the solid phase and in aqueous solution, using a CCD detector. The results showed that the position and width of the major nitrate peak at approximately 1050 cm^{-1} shifted with changes in concentration. It was also demonstrated in the study that the methodology could be used for quantitative detection of nitrates in aqueous solution based on detection of the Raman characteristic peak shift rather than peak intensity.

Additionally, SERS coupled with a commercially available gold nanosubstrate made of a gold-coated silicon material was used in detection of nitrates in water and wastewater by Gajaraj et al. (94). Compared with common Raman spectroscopy, applications of SERS coupled with gold nanosubstrates resulted in enhancement of Raman signals by a factor of $\sim 10^4$. The methodology used in this study was able to detect concentrations of nitrates ranging from 1–10^4 ppm NO_3^- in water samples and 1–100 ppm NO_3^- in wastewater samples. The data obtained showed that the limit of nitrate detection was approximately 0.5 ppm in water and wastewater samples. The results also revealed that SERS coupled with nanosubstrates offers be a promising method for real-time, rapid, and quantitative determination of nitrate concentrations in water and wastewater.

Based on Raman spectroscopy, Kauffmann et al. (95) described a method for quantitative detection of the concentration of inorganic salts in aqueous solutions. The procedure is applied to determine the concentration of sodium nitrate ($NaNO_3$) solutions with a range of 0–100 mM (mmol/L). The data obtained in the experiment showed that the large characteristic peak of the Raman spectrum of a sodium nitrate solution at 1047 cm^{-1} was present in all nitrate solutions and corresponded to the main vibrational mode of NO_3^-. Several spectral processing and normalization methods were used to obtain the best concentration calibration. The limits of detection and quantification were found to be 0.9 mm and 3 mm, respectively.

Nitrite

Nitrite widely exists in such water environments as rivers, lakes, mineral water, drinking water, and aquaculture water, and nitrite is an essential intermediate in the biological nitrogen cycle. However, nitrite is undesirable in the water environment because of its toxicity. The nitrogen fertilizers used in agriculture are primarily responsible for the production of nitrite in the water environment (96). Nitrite is a significant factor in various diseases in aquaculture and could be considered harmful to the human body if present in drinking water. For example, nitrite can promote irreversible oxidization of haemoglobin and reduce the blood's ability to transport oxygen (97).

Furuya et al. (98) adopted resonance Raman spectroscopy for detection of NO_2^- in water by transforming NO_2^- into a colored product (azo dye) via a chemical reaction.

It was indicated that the detection limit of NO_2^- using resonance Raman spectroscopy was approximately 0.5 pbb, which is an order of magnitude lower than that of the usual colorimetry methods. The results demonstrated that resonance Raman spectroscopy could be applied to determination of NO_2^- in wastewater and treated water samples.

Similarly, Lanoul et al. (99) used UV resonance Raman spectroscopy coupled with an intensified CCD detector for detection of nitrate and nitrite in wastewater in 2002. In the experiment, 204-nm and 230-nm excitation wavelengths were used to excite the UV resonance Raman spectrum of wastewater solutions containing sodium nitrite and nitrate, which were detected in concentrations ranging from 7 μM to 3.5 mM (0.1-50 ppm nitrogen). It was found that the strong bands caused by symmetric N-O stretching vibrations occurred at 1044 cm^{-1} (NO_3^-) and 1325 cm^{-1} (NO_2^-). Lanoul et al. carefully analysed the spectrum from the lowest concentrations of 7, 14, and 35 μM to determine the detection limit for measuring the concentrations of the nitrate/nitrite with UV resonance Raman spectroscopy. The results showed that the limits of detection for nitrate and nitrite was <14 μM (<200 ppb).

Zhang et al. (100) described a method for determination of trace NO_2^- in complex samples such as tap water and lake water using shell-isolated nanoparticle-enhanced Raman spectroscopy (SHINERS) in which the substrate was composed of Au/SiO2 nanoparticles with pinholes based on the diazotization-coupling reaction. The concentration of NO_2^- could be detected indirectly from azo dye. The experimental results showed that linearity was obtained in the range of 0.5–6.0 ppm, and the limits of detection were 0.07, 0.08, and 0.10 ppm at 1137, 1395, and 1432 cm^{-1}, respectively. The RSDs (relative standard deviations) were less than 14.5% for several detections. The SHINERS method provided a rapid, sensitive, and selective tool for quantitative detection of nitrite ions in water environment.

Based on the nitrozation reaction between nitrite and an Rh6G molecular probe, Luo et al. (101) applied the rGO/TAgA/Rh6G sensor to probe the Rh6G concentration changes in the nitrosation reaction. The experiment showed that as the concentration of NO_2^- increased, the SERS peak decreased because of the decrease in Rh6G molecules. Thus, this experiment showed that surface-enhanced Raman spectroscopy, a highly selective and sensitive method, could be used for quantitative detection of nitrite in aqueous solution. The results demonstrated that the Raman characteristic peak occurred at 1505 cm^{-1}, and the SERS intensity was linear in the NO_2^- concentration range of 0.70–72 nM, and the limit of detection was 0.2 nM. Additionally, it was shown that the RSD was in the range of 4.4–7.5%, and the recovery was in the range of 94.8–108% using this method.

Table 4. Limits of detection for ferrocyanides and ferricyanides.

Analyte	Diluent	Analyte concentration range	LOD	Correlation coefficient
$Fe(CN)_6^{3-}$	1 M $NaNO_3$	1.25–10 mM	0.17 nM	0.9998
$Fe(CN)_6^{4-}$	1 M $NaNO_3$	1.25–10 mM	0.11 nM	0.99992
$K_4Fe(CN)_6$	$NaNO_3$	1.5–25%	0.6%	0.9994
$Na_4Fe(CN)_6$	$NaNO_3$	1.5–50%	3.9%	0.994

Others

Various Raman spectroscopy techniques have been applied to the detection of other inorganic pollutants in the water environment. Lombardi et al. (46) developed a method for quantitative and qualitative measurement of ferrocyanides and ferricyanides in aqueous solution using Raman spectroscopy coupled with a CCD detector. The LODs (limit of detection) obtained for ferrocyanides and ferricyanides are reported in Table 4. The data in the experiment showed that Raman spectroscopy coupled with a CCD detector could be used for the detection of ferrocyanides and ferricyanides in a water environment.

Additionally, many reports exist on detection methods for cyanide. Liu et al. (102) used SERS based on an Ag nanoplate-built hollow microsphere for trace detection of cyanide in water. In the experiments, this method was employed for detecting trace KCN molecules in water and displayed high SERS activity, structural stability and good measurement reproducibility. It was found that the Raman characteristic peak was located at 2120 cm^{-1}, corresponding to the C ≡ N stretching mode, and a linear double-logarithm relationship was noted between the intensity of the Raman spectra and the concentration of kalium cyanide in water environment in the range of 0.1–1 ppm. Furthermore, the experimental results showed that the LOD could reach 0.1 pbb. Furthermore, the study presented a suitable and rapid method for quantitative and trace detection of CN^- in water.

Wu et al. (103) used laser Raman spectroscopy to study the Raman spectral characteristics of ammonium thiocyanate, ammonium sulfate, and ammonium thiosulfate and their mixed aqueous solutions. The data obtained from the experiment demonstrated that a linear relationship existed between the concentration of anions and peak intensity or peak area. The results indicated that the Raman characteristic peaks of NH_4SCN, NH_4SO_4, and $(NH_4)_2S_2O_3$ were located at 752 cm^{-1}, 982 cm^{-1}, and 997 cm^{-1} in aqueous solutions, respectively, and the correlation coefficients between the Raman peak area and the concentration were 0.99969, 0.99933, and 0.99941, respectively. This work provided a suitable method for quantitative and qualitative detection of ammonium salt in a water environment.

The detection parameters and performances of several types of inorganics obtained from above papers are listed in Table 5. Compared with different kinds of inorganics, the detection method, detection limit, detection range and peak position are clearly presented in the table.

The studies discussed above have proven the sensitivity, effectiveness, and specificity of Raman spectroscopy for detection of inorganics in a water environment. In these studies, several Raman spectroscopy techniques, including surface-enhanced Raman spectroscopy, micro-Raman spectroscopy, resonance Raman spectroscopy and shell-isolated nanoparticle-enhance Raman spectroscopy, were applied for detection of inorganics, and certain methods were able to achieve notably low detection limits. However, few studies have reported on detection of many inorganics (such as ammonia nitrogen) with complex structures and instability. Therefore, together with more advanced Raman spectroscopy techniques, future studies should contribute to detection methods for other inorganics in water. In addition, Raman spectroscopy could be applied to detection of other pollutants in water environments, such as biological pollutants.

Table 5. Detection parameters and performances of inorganics in water using Raman spectroscopy.

Detection materials	Method	Limit of detection	Detection range	Peak positions	Reference
Perchlorate	Surface-enhanced Raman spectroscopy	ClO_4^-: 0.1 ppb	ClO_4^-: 0.5-10 ppm	ClO_4^-: 934 cm^{-1}	(77)
		ClO_4^-: 5 ppb	ClO_4^-: 1-10^5 ppb	ClO_4^-: 930 cm^{-1}	(78)
		ClO_4^-: 10 ppb	ClO_4^-: 10^{-3}-10^2 ppm	ClO_4^-: 937 cm^{-1}	(79)
Heavy metal	Micro-Raman spectroscopy	N/A	N/A	$Cu(In,Ga)Se_2$: 260 cm^{-1}	(82)
	Surface-enhanced Raman spectroscopy	Mercury (II) ions: 100-500 ppt	Mercury (II) ions: 0.1-2.0 ppb	Mercury (II) ions: 1647 cm^{-1}	(83)
		Arsenic (III) ions: 0.76×10^{-6} ppm	Arsenic (III) ions: 4-300 ppb	Arsenic (III) ions: 1108 cm^{-1}	(84)
		N/A	N/A	HgS: 249.13 cm^{-1}CdS: 299.41 cm^{-1} ZnO: 415.25 cm^{-1}	(85)
Sulfate	Micro-Raman spectroscopy	SO_4^{2-}: 220 ppb	N/A	SO_4^{2-}: 983 cm^{-1}	(24)(86)
	Laser Raman spectroscopy	N/A	Ammonium sulfate: 0.1-1.0 M	Ammonium sulfate: 448, 616, 980, and 1104 cm^{-1}	(87)
	Normal Raman spectroscopy	SO_4^{2-}: 200 ppm	SO_4^{2-}: 2×10^3-7×10^4 ppm	SO_4^{2-}: 980 cm^{-1}	(89)
Nitrate	Normal Raman spectroscopy	$NaNO_3$: 10 mM	N/A	$NaNO_3$: 1050 cm^{-1}	(46)
		$NaNO_3$: 0.9 mM	$NaNO_3$:0-100 mM	$NaNO_3$: 1047 cm^{-1}	(95)
	Surface-enhanced Raman spectroscopy	NO_3^-: 0.5 ppm	NO_3^-: 1-10000 ppm	NO_3^-: 1056 cm^{-1}	(94)
Nitrite	Resonance Raman spectroscopy	NO_2^-: 0.5 pbb	N/A	NO_2^-: 1250 cm^{-1}	(98)
	Ultraviolet resonance Raman spectroscopy	NO_2^-: 14 μM	NO_2^-: 0.1-50 ppm	NO_2^-: 1325 cm^{-1}	(99)
	Shell-isolated nanoparticle-enhanced Raman spectroscopy	NO_2^-: 0.07 ppm; 0.08 ppm;0.10 ppm	NO_2^-: 0.5-6.0 ppm	NO_2^-: 1137 cm^{-1}; 1395 cm^{-1}; 1432 cm^{-1};	(100)
	Surface-enhanced Raman spectroscopy	NO_2^-: 0.2 nM	NO_2^-: 0.70-72 nM	NO_2^-: 1505 cm^{-1}	(101)
Ferrocyanides	Normal Raman spectroscopy	$Fe(CN)_6^{4-}$: 0.11 nM	$Fe(CN)_6^{4-}$: 1.25-10 mM	$Fe(CN)_6^{4-}$: 2056.8 and 2093.8 cm^{-1}	(46)
Ferricyanides	Normal Raman spectroscopy	$Fe(CN)_6^{3-}$: 0.17 nM	$Fe(CN)_6^{3-}$:1.25-10 mM	$Fe(CN)_6^{3-}$: 2135.1 cm^{-1}	(46)
Cyanide	Surface-enhanced Raman spectroscopy	KCN: 0.1 pbb	KCN: 0.1 pbb-1.0 ppm	KCN: 2120 cm^{-1}	(102)
Ammonium salt	Laser Raman spectroscopy	N/A	N/A	NH_4SCN, NH_4SO_4 and $(NH_4)_2S_2O_3$: 752 cm^{-1}, 982 cm^{-1} and 997 cm^{-1}	(103)

Table 6. Detection parameters and performances of biological pollutants in water using Raman spectroscopy.

Detection materials		Method	Limit of detection	Detection range	Peak positions	Reference
Biological pollutants	Waterborne pathogens Bacteria	Normal Raman spectroscopy	1×10^{6} cells /membrane	2.4×10^{6}–2.04×10^{8} cells/ml	2800–3000 cm^{-1}	(105)
		Surface-enhanced Raman spectroscopy	2.5×10^{2} cells/mL	1×10^{2}–1×10^{8} cells/mL	735 cm^{-1}	(106)

Biological pollutants

Biological pollution in water is driven by parasites, bacteria and viruses that can cause various human diseases. Additionally, biological pollution can have a large influence on the development of aquaculture due to deterioration of water quality, which could sicken or kill large amounts of fish, shrimp, shellfish, and crabs.

Many reports exist on the detection of biological pollutions using Raman spectroscopy. Stewart et al. (104) published an article describing a method for detection of pathogens in water, and the method in this article was used for the detection of cryptosporidia as an example of pathogen. Cryptosporidia, such as protozoan parasite, causes severe disease in humans and animals due to its high contagiousness. The data from the experiment demonstrated that a suitable Raman spectral characteristic (a Raman shift value characteristic of the pathogen) could be employed for identification of the pathogen in a water environment, and the method described herein can be used to detect Raman shift values in the range of 500–3250 cm^{-1}.

Similarly, using Raman spectroscopy, Escoriza et al. (105) studied a rapid and reliable method for detection of waterborne pathogens in a water environment. The experiment showed that the highest intensity of the bacteria spectral bands was obtained in the range of 2800–3000 cm^{-1} and could facilitate detection of low numbers of microorganisms. However, the concentration of pathogens in the water environment was low. The work adopted filtering approaches to water sampling for Raman detection and showed significant background signals from alumina and silver membranes that reduced the method sensitivity. The results showed a good linear relationship between Raman spectroscopy and other quantification methods, including turbidity ($R^2 = 0.92$), plate counts ($R^2 = 0.87$), and dry weight ($R^2 = 0.97$).

Zhou et al. (106) applied surface-enhanced Raman spectroscopy coupled with silver nanoparticles that coated the cell wall of bacteria to detect living bacteria (Escherichia coli) in aqueous solutions. It was found in the experiment that the Raman spectral intensity of bacteria primarily depended on the zeta potential of the cell wall. The experimental results showed that the total detection time was reduced to 10 min, and the limit of the reactant volume was as low as 1 mL. Additionally, it was demonstrated that the method could be used for the discrimination among three strains of Escherichia coli and one strain of Staphylococcus epidermidis via hierarchy cluster analysis. Furthermore, the results indicated that the limit of detection was 2.5×10^{2} cells/mL. In short, the work offered a new method with many advantages, i.e., reduced reaction time, simple handling, low detection limit, and small amount of sample, for highly sensitive and selective detection of bacteria in a water environment.

The above studies showed that Raman spectroscopy could be applied in detection of biological pollutants in a water environment. Table 6 describes the detection parameters for biological pollutants summarized from the above studies. However, the current empirical studies in this area are relatively rare. In the future, studies should be conducted to optimize Raman spectroscopy techniques (particularly surface-enhanced Raman spectroscopy) such that additional biological pollutants could be detected.

Conclusion and future prospects

A number of preliminary publications on the applications of Raman spectroscopy to the field of water quality detection have been discussed in this article. As described here, various Raman spectroscopy techniques have been widely applied for detection of different contaminants in water environments, including organics, inorganics, and biological contaminants. Additionally, the associated analytical data, including materials, detection methods, limits of detection, detection ranges, peak positions, and selectivity, are presented in detail in this article. Furthermore, combined with advanced Raman technology and Raman instrumentation, Raman spectroscopy has developed into a rapid and accurate tool for quantitative and qualitative detection of materials that have negative influences on water quality.

Although these studies show the capability of Raman spectroscopy in detection of contaminants in a water environment, the application of Raman spectroscopy in the detection of water quality is still beset with difficulties. One of the main challenges is the detection limit. The limits of detection reported in the literature could reach the level of ppm, but much of the allowable concentration range should be at the level of ppb. Additionally, a few of the experiments at the level of ppm were performed in the laboratory instead of in real water environments, which are complex and composed of a large amount of pollutants. Another challenge is that the spectrum of some pollutants in water are difficult to detect. On the one hand, it is known that Raman scattering cross section is 10^{-14} times as large as that of fluorescence scattering cross section, so the spectrum is easier to be buried in the fluorescence. On the other hand, the concentration variation of some common ions particularly anions in a water environment have bad significant interferences on the measurement. Besides, Raman spectroscopy has higher variation in determining pollutants for different researchers due to its work procedures, which could be affected by many factors, including various Raman spectroscopy, sample preparation, laser light intensity, and Raman instrumental settings.

Therefore, further works based on Raman spectroscopy is required to find which kind of Raman spectroscopy technique is the most suitable method for detection of various of pollutants in a water environment. Additionally, progress is needed in the area of instrumentation that involves more suitable excitation light sources, greater stability, and accuracy of detectors, more exact and rapid data processing systems, and spectrometers with greater portability. Moreover, the combination of RRS, SERS, micro-Raman spectroscopy, and near infrared Raman spectroscopy, and the use of nonlinear Raman spectroscopy (i.e., stimulated Raman spectroscopy, inverse Raman spectroscopy, and coherent anti-Stokes Raman spectroscopy) would lead to new breakthroughs in rapid, on-line and quantitative detection of water quality.

Acknowledgments

We would like to thank Molly G. for providing an English-language edit of this article.

Funding

The authors are grateful for financial support from the National Natural Science Foundation of China (Grant no. 61571444).

References

1. Bartram, J. and Ballance R. (2003) Water quality monitoring: A practical guide to the design and implementation of freshwater quality studies and monitoring programmes. *J. Tratamento Da Àgua* 55 (2): 1–37.
2. Shannon, M.A., Bohn, P.W., Elimelech, M., Georgiadis, J.G., Mariñas, B.J., and Mayes, A.M. (2008) Science and technology for water purification in the coming decades. *J. Nat.* 452 (7185): 301–310.
3. United Nations Environment Progrmme. (2007) *UNEP year book*. M. United Nations Environment Progrmme, Naibi, Kenya.
4. Gowen, A.A., Tsenkova, R., Bruen, M., and O'Donnell, C. (2012) Vibrational spectroscopy for analysis of water for human use and in aquatic ecosystems. *J. Crit. Rev. Env. Sci. Tec.* 42 (23): 2546–2573(28).
5. Hasan, J., Goldbloom-Helzner, D., Ichida, A., Rouse, T., and Gibson, M. (2005) *Technologies and techniques for early warning systems to monitor and evaluate drinking water quality: A state-of-the-art review*. United States Environmental Protection Agency, Washington, DC.
6. Bardow, A., Marquardt, W., GÖke, V., Koss, H., and Lucas, K. (2003) Model-based measurement of diffusion using Raman spectroscopy. *Aiche J.* 49 (2): 323–334.
7. Denuault, G. (2009) Electrochemical techniques and sensors for ocean research. *J. Ocean Sci.* 5 (2): 1857–1893.
8. Rastogi, P.K., Ganesan, V., and Krishnamoorthi, S. (2013) A promising electrochemical sensing platform based on a silver nanoparticles decorated copolymer for sensitive nitrite determination. *J. Mater. Chem. A* 2 (4): 933–943.
9. Abbas, M.N. and Mostafa, G.A. (2000) Determination of traces of nitrite and nitrate in water by solid phase spectrophotometry. *J. Anal. Chim. Acta* 410: 185–192(8).
10. Pashkova, G.V. and Revenko, A.G. (2015) A review of application of total reflection X-ray fluorescence spectrometry to water analysis. *J. Appl. Spectrosc. Rev* 50 (6): 443–472.
11. Chen, J. and Teo, K.C. (2001) Determination of cadmium, copper, lead and zinc in water samples by flame atomic absorption spectrometry after cloud point extraction. *J. Anal. Chim. Acta* 450 (1-2): 215–222.
12. Rahmelow, K. and Hubner, W. (1997) Infrared spectroscopy in aqueous solution: difficulties and accuracy of water subtraction. *J. Appl. Spectrosc*, 51 (2): 160–170.
13. Fang, L., Wu, J., and Su Y.L. (2008) Determination of perchlorate in drinking water using ion chromatography. *J. Guangdong Trace Elements Sci.* 15 (12): 61–63.
14. Bradley, E.B. and Frenzel, C.A. (1970) On the exploitation of laser Raman spectroscopy for detection and identification of molecular water pollutants. *J. Water Res.* 4: 125–128.
15. Zhao, Y.L., Zhao, D.A., and Li, D.L. (2015) Electrochemical and other methods for detection and determination of dissolved nitrite: a review. *Int. J. Electrochem. Sci.* 10: 1144–1168.
16. Zhu, X., Xu, T., Lin, Q., and Duan, Y. (2013) Technical development of Raman spectroscopy: from instrumental to advanced combined technologies. *J. Appl. Spectrosc. Rev.* 49 (1): 64–82.
17. Bowen, J.M., Sullivan, P.J., Blanche, S.M., Essington, M., and Noe, L.J. (1989) Optical-fiber Raman spectroscopy used for remote in-situ environmental analysis. P. USdoi: US4802761 A.
18. Potgieter-Vermaak, S.S., Potgieter, J.H., and Van Grieken, R. (2006) The application of Raman spectrometry to investigate and characterize cement, Part I: A review. *J. Cem. Concr. Res.* 36 (4): 656–662.
19. Smekal, A. (1923) Zur quantentheorie der dispersion. *J. Naturwissenschaften* 11 (43): 873–875.
20. Raman, C.V. and Krishnan, K.S. (1928) A new type of secondary radiation. *J. Nat.* 121 (3048): 501–502.
21. Glockler, G. (1930) The Raman effect. *J. Scientif. Month.* 31 (4): 361–367.

22. Talari, A.C.S., Movasaghi, Z., Rehman, S., and Rehman, I. (2015) Raman spectroscopy of biological tissues. *J. Appl. Spectrosc. Rev* 50(1), 46–111.
23. Heller, E.J., Sundberg, R., and Tannor, D. (1982) Simple aspects of Raman scattering. *J. Phys. Chem.* 86 (10):1822–1833.
24. Burke, E.A.J. (2001) Raman microspectrometry of fluid inclusions. *J. Lithos* 55 (1): 139–158.
25. Roberts, S. and Beattie, I. (1995) Micro-Raman spectroscopy in the earth sciences. In *Microprobe techniques in the Earth*, Potts, P.J., Bowles, J.F., Reed, S.J., Cave. R., Eds., Sciences Springer, New York, pp. 387–408.
26. McMillan, P. 1985. Vibrational spectroscopy in the mineral sciences. *J. Rev. Minera* 14: 9–63.
27. McMillan, P.F. (1989) Raman spectroscopy in mineralogy and geochemistry. *J. Ann. Rev. Earth Planet. Sci.* 17: 225–283.
28. Stokes, R.J. (2008) Surface-enhanced Raman scattering spectroscopy as a sensitive and selective technique for the detection of folic acid in water and human serum. *J. Appl. Spectrosc.* 62 (4): 371–376(6).
29. Luo, B.S. and Lin, M. (2008) A portable Raman system for the identification of foodborne pathogenic bacteria. *J. Rapid Meth. Aut. Mic.* 16 (3): 238–255.
30. Li, Z.Y., Deen, M.J., Kumar, S., and Selvaganapathy, P.R. (2014) Raman spectroscopy for in-line water quality monitoring–instrumentation and potential. *J. Sens. Basel, Switzerland* 14 (9): 17275–17303.
31. Kogelnik, H. and Porto, S. (1963) Continuous helium-neon red laser as a Raman source. *J. Opt. Soc. Am.* 53: 1446–1447.
32. Hirschfeld, T. and Chase, B. (1986) FT-Raman spectroscopy: Development and justification. *J. Appl. Spectrosc.* 40: 133–137.
33. Song, K., Lee, Y.I., and Sneddon, J. (2007) Recent developments in instrumentation for laser induced breakdown spectroscopy. *J. Appl. Spectrosc. Rev.* 37 (1): 89–117.
34. Lewis, I.R. and Edwards, H. (2001) *Handbook of Raman spectroscopy: From the research laboratory to the process line*. Marcel Dekker, Basel, Switzerland.
35. Das, R.S. and Agrawal, Y.K. (2011) Raman spectroscopy: Recent advancements, techniques and applications. *J. Vib. Spectrosc.* 57 (2): 163–176.
36. Murray, C. and Dierker, S. (1986) Use of an unintensified charge-coupled device detector for low-light-level Raman spectroscopy. *J. Opt. Soc. Am. A.* 3 (12): 2151–2159.
37. Hardy, T.D., Deen, M.J., and Murowinski, R.G. (1999) Effects of radiation damage on scientific charge coupled devices. *J. Adv. Imaging Electron Phys.* 106: 1–96.
38. Wu, Q., Hamilton, T., Nelson, W.H., Elliott, S., Sperry, J.F., and Wu, M. (2001) UV Raman spectral intensities of E. coli and other bacteria excited at 228.9, 244.0, and 248.2 nm. *J. Anal. Chem.* 73: 3432–3440.
39. Deen, M.J. and Basu, P.K. (2012) *Silicon Photonics—Fundamentals and Devices*. John Wiley and Sons Ltd.: Chichester, UK.
40. Kumar, S. and Deen, M.J. (2014) *Fiber optic communications—Fundamentals and applications*. John Wiley and Sons Ltd., Chichester, UK.
41. Grossmann, A., and Morlet, J. (1984) Decomposition of hardy functions into square integrable wavelets of constant shape. *J. Siam J. Math. Anal.* 15 (4): 723–736.
42. Robert, B. (2009) Resonance Raman spectroscopy. *J. Photosynth Res.* 101: 147–155.
43. Campion, A. and Kambhampati, P. (1998) Surface-enhanced Raman scattering. *J. Chem. Soc. Rev.* 27 (4): 241–250.
44. Chase, B. (1987) Fourier transform Raman spectroscopy. *J. Microchim. Acta* 93 (1–6): 81–91.
45. Tseng, C.H., Mann, C.K., and Vickers, T.J. (1993) Determination of organics on metal surfaces by Raman spectroscopy. *J. Appl. Spectrosc.* 47 (11): 1767–1771.
46. Lombardi, D.R., Wang, C., Sun, B., Fountain, A.W., Vickers, T.J., and Mann, C.K. (1994) Quantitative and qualitative analysis of some inorganic compounds by Raman spectroscopy. *J. Appl. Spectrosc.* 48 (7): 875–883.
47. Leyton, P., Sanchez-Cortes, S., Garcia-Ramos, J.V., Domingo, C., Campos-Vallette, M., and Saitz, C. (2004) Selective molecular recognition of polycyclic aromatic hydrocarbons (PAHs) on calix

[4]arene-functionalized Ag nanoparticles by surface-enhanced Raman scattering. *J. Phys. Chem. B* 108 (45): 17484–17490.
48. Carrasco, E.A., Campos-Vallette, M., Leyton, P., Diaz, G., Clavijo, R.E., García-Ramos, J.V., Inostroza, N., Domingo, C., Sanchez-Cortes, S., and Koch, R. (2003) Study of the interaction of pollutant nitro polycyclic aromatic hydrocarbons with different metallic surfaces by surface-enhanced vibrational spectroscopy (SERS and SEIR). *J. Phys. Chem. A* 107 (45): 9611–9619.
49. Schmidt, H., Ha, N.B., Pfannkuche, J., Amann, H., Kronfeldt, H.D., and Kowalewska, G. (2004) Detection of PAHs in seawater using surface-enhanced Raman scattering (SERS). *J. Mar. Pollut. Bull.* 49 (3): 229–234.
50. Costa, J.C., Sant'Ana, A.C., Corio, P., and Temperini, M.L. (2006) Chemical analysis of polycyclic aromatic hydrocarbons by surface-enhanced Raman spectroscopy. *J. Talanta* 70 (5): 1011–1016.
51. Xie, Y.F., Wang, X., Han, X.X., Song, W., Ruan, W.D., and Liu, J.Q., Zhao, B., and Ozaki, Y. (2011) Selective SERS detection of each polycyclic aromatic hydrocarbon (PAH) in a mixture of five kinds of PAHs. *J. Raman Spectrosc.* 42 (5): 945–950.
52. Leyton, P., Domingo, C., Sanche-Cortes, S., Campos-Vallette, M., and Garcia-Ramos, J.V. (2005) Surface enhanced vibrational (IR and Raman) spectroscopy in the design of chemosensors based on ester functionalized p-tert-butylcalix [4]arene hosts. *J. Langmuir* 21 (25): 11814–11820.
53. Leyton, P., Sanche-Cortes, S., Campos-Vallette, M., Domingo, C., Garcia-Ramos, J.V., and Saitz, C. (2005) Surface-enhanced micro-Raman detection and characterization of calix [4]arene-polycyclic aromatic hydrocarbon host-guest complexes. *J. Appl. Spectrosc.* 59 (8): 1009–1015.
54. Guerrini, L., Garcia-Ramos, J.V., Domingo, C., and Sanchez-Cortes, S. (2009) Sensing polycyclic aromatic hydrocarbons with dithiocarbamate-functionalized Ag nanoparticles by surface-enhanced Raman scattering. *J. Anal. Chem.* 81 (3): 953–960.
55. Shi, X., Kwon, Y., Ma, J., Zheng, R., Wang, C., and Kronfeldt, H. (2013) Trace analysis of polycyclic aromatic hydrocarbons using calixarene layered gold colloid film as substrates for surface-enhanced Raman scattering. *J. Raman Spectrosc.* 44 (1): 41–46.
56. Kwon, Y.H., Sowoidnich, K., Schmidt, H., and Kronfeldt, H.D. (2012) Application of calixarene to high active surface-enhanced Raman scattering (SERS) substrates suitable for in situ detection of polycyclic aromatic hydrocarbons (PAHs) in seawater. *J. Raman Spectrosc.* 43 (8): 1003–1009.
57. Qu, L.L., Li, Y.T., Li D.W., Xue J.Q., Fossey J.S., and Long Y.T. (2013) Humic acids-based one-step fabrication of SERS substrates for detection of polycyclic aromatic hydrocarbons. *J. Analyst* 138 (5): 1523–1528.
58. López-Tocón, I., Otero, J.C., Arenas, J.F., Garcia-Ramos, J.V., Sanchez-Cortes, S., and Chem, A. (2011) Multicomponent direct detection of polycyclic aromatic hydrocarbons by surface-enhanced Raman spectroscopy using silver nanoparticles functionalized with the viologen host lucigenin. *J. Anal. Chem.* 83 (7): 2518–2525.
59. Howlett, L.E. (1931) Raman spectra of benzene and toluene. *J. Nat.* (3236): 796.
60. Liu, Q.C., Wu, Q.Y., Mu, Y.Q., Lan F.Y., and Shi, L. (2009) Studying the laser Raman spectroscopy for benzene and carbon tetrachloride. *J. HuaiBei Coal Industr. Teach. School (Nat. Sci.)* 30 (2): 17–20.
61. Ma, J. and Huang, R. (2014) Low-concentration detection of benzene using laser Raman spectroscopy. *J. Opt. Tech.* 40 (3): 195–198.
62. Huang, R., Ma, J., and Shi, Y. (2012) The study of color-benzene by using laser Raman spectroscopy. *J. Fuzhou Univ.* 40 (1): 58–62.
63. Tao, J.Y., Dai-Sheng, X.U., Mei, X.A., and Mao, L.X. (2010) Laser-Raman spectrum for detecting benzene. *J. Appl. Opt.* 31 (2): 273–276.
64. Iliescu, T., Baia, M., and Pavel, I. (2006) Raman and SERS investigations of potassium benzylpenicillin 69. *J. Raman Spectrosc.* 37 (1–3): 318–325.
65. He, L., Lin, M., Li, H., and Kim, N.J. (2010) Surface-enhanced Raman spectroscopy coupled with dendritic silver nanosubstrate for detection of restricted antibiotics. *J. Raman Spectrosc.* 41 (7): 739–744.

66. Ma, J., Kong, D.D., Han, X.H., Guo, W.L., and Shi, X.F. (2013) Detection of antibiotics in water using silver colloid films as substrate of surface-enhanced Raman scattering. *J. Spectrosc. Spect. Anal.* 33 (10): 2688–2693(6).
67. Strickland, A.D., Batt, C.A., and Chem., A. (2009) Detection of carbendazim by surface-enhanced Raman scattering using cyclodextrin inclusion complexes on gold nanorods. *J. Anal. Chem.* 81 (8): 2895–2903.
68. Wang, X.T., Shi, W.S., She, G.W., Mu, L.X., and Lee, S.T. (2010) High-performance surface-enhanced Raman scattering sensors based on Ag nanoparticles-coated Si nanowire arrays for quantitative detection of pesticides. *J. Appl. Phys. Lett.* 96 (5): 053104-053104-3.
69. Yazdi, S.H. and White, I.M. (2013) Multiplexed detection of aquaculture fungicides using a pump-free optofluidic SERS microsystem. *J. Analyst* 138 (1): 100–103.
70. Kubackova, J., Fabriciova, G., Miskovsky, P., Jancura, D., and Sanchez-Cortes, S. (2015) Sensitive surface-enhanced Raman spectroscopy (SERS) detection of organochlorine pesticides by alkyl dithiol-functionalized metal nanoparticles-induced plasmonic hot spots. *J. Anal. Chem.* 87 (1): 663–669.
71. Marley, N.A., Mann, C.K., and Vickers, T.J. (1984) Determination of phenols in water using Raman spectroscopy. *J. Appl. Spectrosc.* 38 (4): 540–542.
72. Si, M.Z., Kang, Y.P., and Liu, R.M. (2012) Surface-enhanced Raman scattering (SERS) spectra of three kinds of azo-dye molecules on silver nanoparticles prepared by electrolysis. *J. Appl. Surf. Sci*, 258 (15): 5533–5537.
73. Tanner, P.A. and Leung, K.H. (1996) Spectral interpretation and qualitative analysis of organophosphorus pesticides using FT-Raman and FT-infrared spectroscopy. *J. Appl. Spectrosc.* 50 (5): 565–571.
74. Williams, T.L., Martin, R.B., and Collette, T.W. (2001) Raman spectroscopic analysis of fertilizers and plant tissue for perchlorate. *J. Appl. Spectrosc.* 55 (8): 967–983.
75. Martinelango, P.K., Anderson, J.L., Dasgupta, P.K., Armstrong, D.W., Al-Horr, R.S., and Slingsby, R. (2005) Gas-phase ion association provides increased selectivity and sensitivity for measuring perchlorate by mass spectrometry. *J. Anal. Chem.* 77 (15): 4829–4835.
76. Li, Y.T., George, E.J., and Chem, A. (2005) Analysis of perchlorate in water by reversed-phase lc/esi-ms/ms using an internal standard technique. *J. Anal. Chem.* 77 (14): 4453–4458.
77. Ruan, C.M., Wang, W., and Gu, B.H. (2006) Surface-enhanced Raman scattering for perchlorate detection using cystamine-modified gold nanoparticles. *J. Anal. Chem. Acta* 567 (1): 114–120.
78. Hao, J.M., Xu, Z.H., Han, M.J., Xu, S.Y., and Meng, X.G. (2010) Surface-enhanced Raman scattering analysis of perchlorate using silver nanofilms deposited on copper foils. *J. Colloid. Surface. A.* 366 (1–3): 163–169.
79. Li L.X., Huang, J., Chen, N., Liu, S.P., and Chen Z.Y. (2013) Detection of perchlorate ion using surface-enhanced Raman spectroscopy technology. *J. Environ. Pollut. Control* 35 (8): 20–22.
80. Milićević, D.R., Jovanović, M., Petrović, Z., and Stefanović, M. (2009) Toxicological assessment of toxic element residues in swine kidney and its role in public health risk assessment. *J. Inter. J. Env. Res. Pub. Heal.* 6 (12): 3127–3142.
81. Chipasa, K.B. (2003) Accumulation and fate of selected heavy metals in a biological wastewater treatment system. *J. Waste Manage.* 23 (2): 135–143.
82. Witte, W., Kniese, R., and Powalla, M. (2008) Raman investigations of Cu (In, Ga) Se_2 thin films with various copper contents. *J. Thin Solid Films* 517 (2): 867–869.
83. Wang, G., Lim, C., Chen, L., Chon, H., Choo, J., and Hong, J., and Demello, A.J. (2009) Surface-enhanced Raman scattering in nanoliter droplets: Towards high-sensitivity detection of mercury (ii) ions. *J. Anal. Bioanal. Chem.* 394 (7): 1827–1832.
84. Li, J., Chen, L.X., Lou, T., and Wang, Y.Q. (2011) Highly sensitive SERS detection of As^{3+} ions in aqueous media using glutathione functionalized silver nanoparticles. *J. Acs Appl. Mater. Inter.* 3 (10): 3936–3941.
85. Eshkeiti, A., Narakathu, B.B., Reddy, A.S. G., Moorthi, A., and Atashbar, M.Z. (2011) A novel inkjet printed surface enhanced Raman spectroscopy (SERS) substrate for the detection of toxic heavy metals. *J. Procedia Eng.* 25 (35): 338–341.

86. Dubessy, J., Moissette, A., Bakker, R.J., Frantz, J.D., and Zhang, Y.G. (1999) High-temperature Raman spectroscopic study of H 2 O-CO 2 -CH 4 mixtures in synthetic fluid inclusions; first insights on molecular interactions and analytical implications. *J. Eur. J. Min.* 11 (1): 23–32.
87. Sun, S., Cai, Y.D., Liu, Y., Wang J.J., Ye, Y., and Chen, S.H. (2014) Research on Raman spectral characteristics and mechanism of ammonium sulfate solution. *J. Acta Opt. Sin.* 34 (3): 315–319.
88. Zou, X.Y., Lv, X.B., and He, M.C. (2007) Quantitative Analysis of Common Acid Radical Ions by Laser Raman Spectrometry. *J. Rock Minera. Anal.* 26 (1): 26–28.
89. Deng, X.B., Chen, M., Liu, C.L., Ren, H.B., and Zhuang, X.G. (2014) Quantitative determination of sulfate in hydrate and water systems by Raman spectrometry. *J. Rock Minera. Anal.* 33 (3): 413–418.
90. Vitousek, P.M., Aber, J.D., Howarth, R.W., Likens, G.E., Matson, P.A., Schindler, D.W., Schlesinger W.H., and Tilman, G.D. (1997) Human alteration of the global nitrogen cycle: Sources and consequences. *J. Ecol. Appl.*, 7 (3), 737–750.
91. Camargo, J.A., Alonso, A., and Salamanca, A. (2005) Nitrate toxicity to aquatic animals: A review with new data for freshwater invertebrates. *J. Chemosphere* 58 (9): 1255–1267.
92. Jensen, F.B. (2003) Nitrite disrupts multiple physiological functions in aquatic animals. *J. Comp. Biochem. Phys. A.* 135 (1): 9–24.
93. Greer, F.R., and Shannon, M. (2005) Infant methemoglobinemia: the role of dietary nitrate in food and water. *J. Pediatrics* 116 (3): 784–786.
94. Gajaraj, S., Fan, C., Lin, M., and Hu, Z. (2013) Quantitative detection of nitrate in water and wastewater by surface-enhanced Raman spectroscopy. *J. Environ. Monit. Assess.* 185 (7): 5673–5681.
95. Kauffmann, T.H. and Fontana, M.D. (2015) Inorganic salts diluted in water probed by Raman spectrometry: data processing and performance evaluation. *J. Sensor. Actuat. B-Chem.* 209: 154–161.
96. Gopalan, A.I., Lee, K.P., and Komathi, S. (2010) Bioelectrocatalytic determination of nitrite ions based on polyaniline grafted nanodiamond. *J. Biosens. Bioelectron.* 26 (4): 1638–1643.
97. Wang, P., Mai, Z.B., Dai, Z., Li, Y.X., and Zou, X.Y. (2009) Construction of Au nanoparticles on choline chloride modified glassy carbon electrode for sensitive detection of nitrite. *J. Biosens. Bioelectron.* 24 (11): 3242–3247.
98. Furuya, N., Matsuyuki, A., Higuchi, S., and Tanaka, S. (1980) Determination of nitrite ion in waste and treated waters by resonance Raman spectrometry. *J. Water Res.* 14 (7): 747–752.
99. Lanoul, A. (2002) Uv resonance Raman spectroscopic detection of nitrate and nitrite in wastewater treatment processes. *J. Anal. Chem.* 74 (6): 1458–1461.
100. Zhang, K.G., Hu, Y.L., and Li, G.K. (2013) Diazotization-coupling reaction-based selective determination of nitrite in complex samples using shell-isolated nanoparticle-enhanced Raman spectroscopy. *J. Talanta* 116 (22): 712–718.
101. Luo, Y.H., Wen, G.Q., Dong, J.C., Liu, Q.Y., Liang, A.H., and Jiang, Z.L. (2014) SERS detection of trace nitrite ion in aqueous solution based on the nitrosation reaction of rhodamine 6g molecular probe. *J. Sensor. Actuat. B-Chem.* 201 (4): 336–342.
102. Liu, G.Q., Cai, W.P., Kong, L.C., Duan, G.T., Li, Y., Wang, J.J., and Chen Z.X. (2013) Trace detection of cyanide based on SERS effect of Ag nanoplate-built hollow microsphere arrays. *J. J. Hazard. Mater.*, 248–249 (6): 435–441.
103. Wu, Q. (2013) *Researching on the Raman spectra characteristics and quantitative analysis of compound ammonium salt*. D. Jiangsu Normal University, pp. 1–65.
104. Grow A.E., Wood L.L., Claycomb J.L., and Thompson, P.A. (2003) New biochip technology for label-free detection of pathogens and their toxins. *J. Microbiol. Meth.* 53 (2): 221–233.
105. Escoriza, M.F., VanBriesen, J.M., Stewart, S., Maier, J., and Treado, P.J. (2006) Raman spectroscopy and chemical imaging for quantification of filtered waterborne bacteria. *J. Microbiol. Meth*, 66 (1): 63–72.
106. Zhou, H.B., Yang, D.T., Lvleva, N.P., Mircescu, N.E., Niessner, R., and Haisch, C. (2014) SERS detection of bacteria in water by in situ coating with Ag nanoparticles. *J. Anal. Chem.* 86 (3): 1525–1533.